Report

A Bio-Inspired Flying Robot Sheds Light on Insect Piloting Abilities

Nicolas Franceschini,[1,*] Franck Ruffier,[1]
and Julien Serres[1]
[1] Biorobotics Lab
Movement and Perception Institute
Centre National de la Recherche Scientifique and
University of the Mediterranean
163 Avenue de Luminy, CP938
Marseille F-13288, cedex 9
France

Summary

When insects are flying forward, the image of the ground sweeps backward across their ventral view-field and forms an "optic flow," which depends on both the groundspeed and the groundheight. To explain how these animals manage to avoid the ground by using this visual motion cue, we suggest that insect navigation hinges on a visual-feedback loop we have called the *optic-flow regulator,* which controls the vertical lift. To test this idea, we built a micro-helicopter equipped with an optic-flow regulator and a bio-inspired *optic-flow sensor.* This fly-by-sight micro-robot can perform exacting tasks such as take-off, level flight, and landing. Our control scheme accounts for many hitherto unexplained findings published during the last 70 years on insects' visually guided performances; for example, it accounts for the fact that honeybees descend in a headwind [1], land with a constant slope [2], and drown when travelling over mirror-smooth water [3]. Our control scheme explains how insects manage to fly safely without any of the instruments used onboard aircraft to measure the groundheight, groundspeed, and descent speed. An optic-flow regulator is quite simple in terms of its neural implementation and just as appropriate for insects as it would be for aircraft [4].

Results and Discussion

According to Kennedy's "optomotor theory," flying insects have a "preferred" retinal velocity with respect to the ground below [5, 6]. In response to wind, for example, they may adjust their groundspeed or ground-height to restore the apparent velocity of the ground features. This insightful theory has left a rather confusing picture in its wake, however, because it was never translated into a control scheme, which would have brought to light the various flight variables involved, the sensors required, the dynamics of the various system components, and the causal links between the sensors and the variables to be controlled. Questions therefore arise as to which variable(s) the insect actually *measures* and

*Correspondence: nicolas.franceschini@univmed.fr

which one(s) it *controls* to avoid the ground on the basis of the optic flow (OF).

The "ventral optic flow" perceived by the insect, i.e., the apparent angular velocity ω created by a point directly below on the flight track, is simply equal to the ratio between groundspeed v_x and the groundheight h (Figure 1A), as follows:

$$\omega = v_x/h \ [\text{rad} \cdot \text{s}^{-1}] \qquad (1)$$

Flies and bees are able to measure the angular velocity ω of the surroundings irrespective of the spatial texture and contrast [7–10], and some of their neurones respond monotonically to ω [11, 12]. Neurones facing downwards can therefore act as ventral OF sensors and thus estimate the ratio v_x/h (Figure 1).

We recently developed a simple OF-based autopilot that enables a robotic micro-helicopter (MH) to perform challenging tasks such as take-off, terrain following, and landing [4]. The crux of our autopilot is an *OF sensor* that measures the ventral OF and a feedback loop called the OF regulator (Figure 2A), which strives to maintain ω constant and equal to a set-point ω_{set}. A comparator produces an error signal, $\varepsilon = \omega_{meas} - \omega_{set}$, which drives a controller adjusting the lift, and thus the groundheight, so as to minimize ε. All the operator does is to set the pitch angle Θ (Figure 2B); the OF regulator does the rest, including keeping the $v_x{:}h$ ratio constant in the steady state:

$$v_x/h = \omega \approx \omega_{meas} \approx \omega_{set} = \text{constant} \qquad (2)$$

We tested the idea that insects may be equipped with a similar OF regulator by comparing the behavior of insects with that of the robot in similar situations. Our control scheme (Figure 2), which produces the micro-robot's behavioral pattern (Figure 3), was found to account for a series of puzzling, seemingly unconnected flying abilities observed by many authors over the last 70 years in various species (fruit flies, locusts, honeybees, moths, mosquitoes, dung beetles, and butterflies).

1. Take-off

An insect that increases its forward thrust (e.g., by pitching forward like a fly [13], a bee [14], or a helicopter: Figure 2B) is bound to ascend if it is equipped with the OF regulator shown in Figure 2A because the feedback loop constantly increases the groundheight h proportionally to the groundspeed v_x to comply with Equation 2. The insect will therefore respond to the slightest deviation ε from the OF set-point simply by adjusting its groundheight.

The performances of the MH illustrate this point quite clearly (Figure 3A, left). Starting at position 1 (with the rotor axis oriented vertically and the lift just balancing the weight), the MH is remotely commanded to pitch "nose down" (Θ from 0° to +10° rampwise). The ensuing acceleration (Figure 3B) automatically causes the micro-flier to rise (Figure 3A) because the feedback loop increases
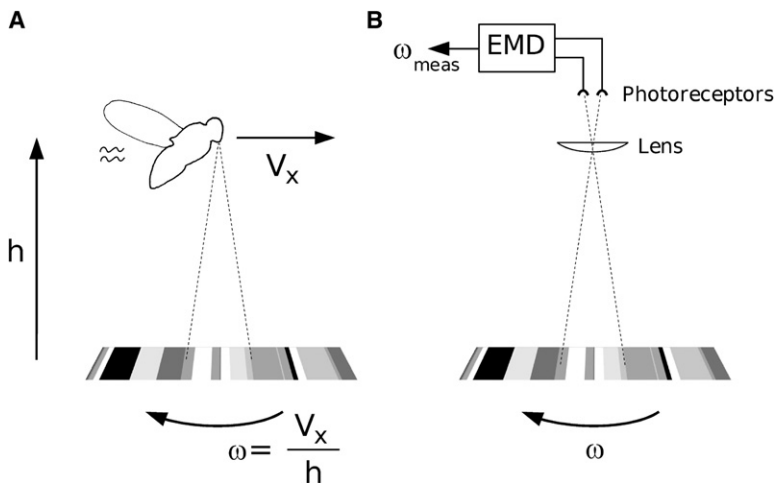
Figure 1. Definition, ω, and Measurement, ω_{meas}, of the Ventral Optic Flow Perceived by an Animal Flying in Translation in the Longitudinal Plane

(A) The ventral OF perceived by an animal flying at groundspeed v_x and groundheight h is the angular speed ω at which a point in the ground texture directly below seems to move in the opposite direction. By definition, ω (in rad/s) is the ratio between groundspeed and groundheight. The one-dimensional randomly textured ground shown here is a magnified sample of that shown below Figure 3A. (B) The minimalistic "OF sensor" used onboard our aerial robot comprises a microlens and two photoreceptors driving a fly-inspired elementary motion detector (EMD). The output ω_{meas} from the OF sensor will serve as a feedback signal in the control scheme shown in Figure 2A.

h in proportion to v_x and thus effectively maintains a relatively constant ω throughout take-off (Figure 3D).

2. Level Flight and Terrain Following

Migrating butterflies crossing narrow canyons fly down into the gully and across the bottom [15]. When the butterflies traverse dense forests, the distance at which they clear the canopy is roughly equal to their previous height above the ground, and once they have crossed this large obstacle, they redescend [16]. High-flying dung beetles have a high groundspeed, whereas the lower fliers adopt a lower speed [17]. These findings illustrate the insect's terrain-following ability and show the existence of a tight link between groundspeed and groundheight (see also Figure 7b in [2]). To keep the OF constant (Equation 2), the insect might either measure its groundspeed (with some kind of "speedometer") and adjust its groundheight proportionately or measure its groundheight (with some kind of "altimeter") and adjust its groundspeed accordingly. Our control scheme (Figure 2A) predicts that an insect will fly at a groundheight proportional to its groundspeed without measuring either of these two variables.

The MH flight pattern illustrates this point. Upon reaching a steady groundspeed of 3 m·s^{-1} (Figure 3B), the MH can be seen to have cruised at a steady
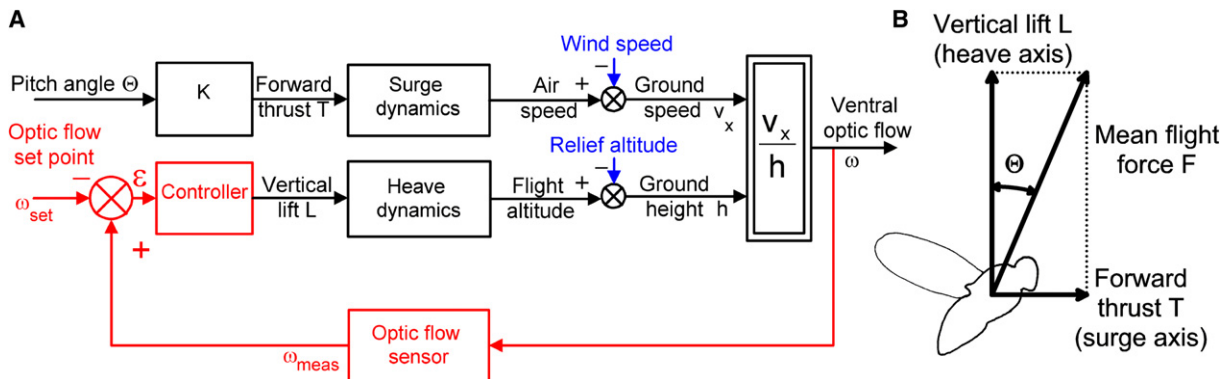

Figure 2. An Optic-Flow Regulator Accounts for Insect Visually Guided Flight Control over the Ground

The OF regulator controls the lift at all times so as to maintain the ventral OF ω constant.
(A) Block diagram of the information flow giving the causal and dynamic relationships between sensory and motor variables. The upper (open-loop) pathway describes how an increase in pitch angle Θ of the mean flight-force vector (see [B]) results in a proportional increase in forward thrust, and thus in groundspeed v_x via the surge dynamics. The bottom (red) pathway shows how the ventral OF is measured (ω_{meas}) and compared with an OF set-point (ω_{set}). The error signal ($\varepsilon = \omega_{meas} - \omega_{set}$) delivered by the comparator drives a controller adjusting the vertical lift L, and thus the groundheight h via the heave dynamics, so as to maintain a constant OF ω (equal to ω_{set}), whatever the groundspeed. The right part of this functional diagram depicts the system dynamics, defines the ventral OF as $\omega = v_x/h$, and shows the points at which two disturbances impinge on the system: the relief altitude subtracted from the flight altitude gives the groundheight; and the wind speed subtracted from (by headwind) or added to (by tailwind) the airspeed gives the groundspeed. Because ω is by definition an inverse function of the controlled variable h (Equation 2), the feedback loop is nonlinear (the nonlinearity is symbolized by the two nested rectangles). The controller includes proportional and derivative (PD) functions, which ensure closed-loop stability in the groundspeed range of 0–3 m/s.
(B) Like flies [13, 23, 34–37], bees [14] and full-scale helicopters, our MH gains speed by pitching its mean flight-force vector forward at a small angle Θ with respect to the vertical. The mean flight force F of the MH results from the rotor speed and can be resolved into vertical lift L and forward thrust T. However, any change in F will mainly affect L (for two reasons: see Experimental Procedures). In flies, the mean flight-force vector orientation differs from the body orientation, forming a fixed angle [13, 23, 34, 35]. Other insects, such as hoverflies, have a more complicated flight-control system [38], but the OF-regulation principle proposed here operates whatever the mechanism producing the forward thrust.
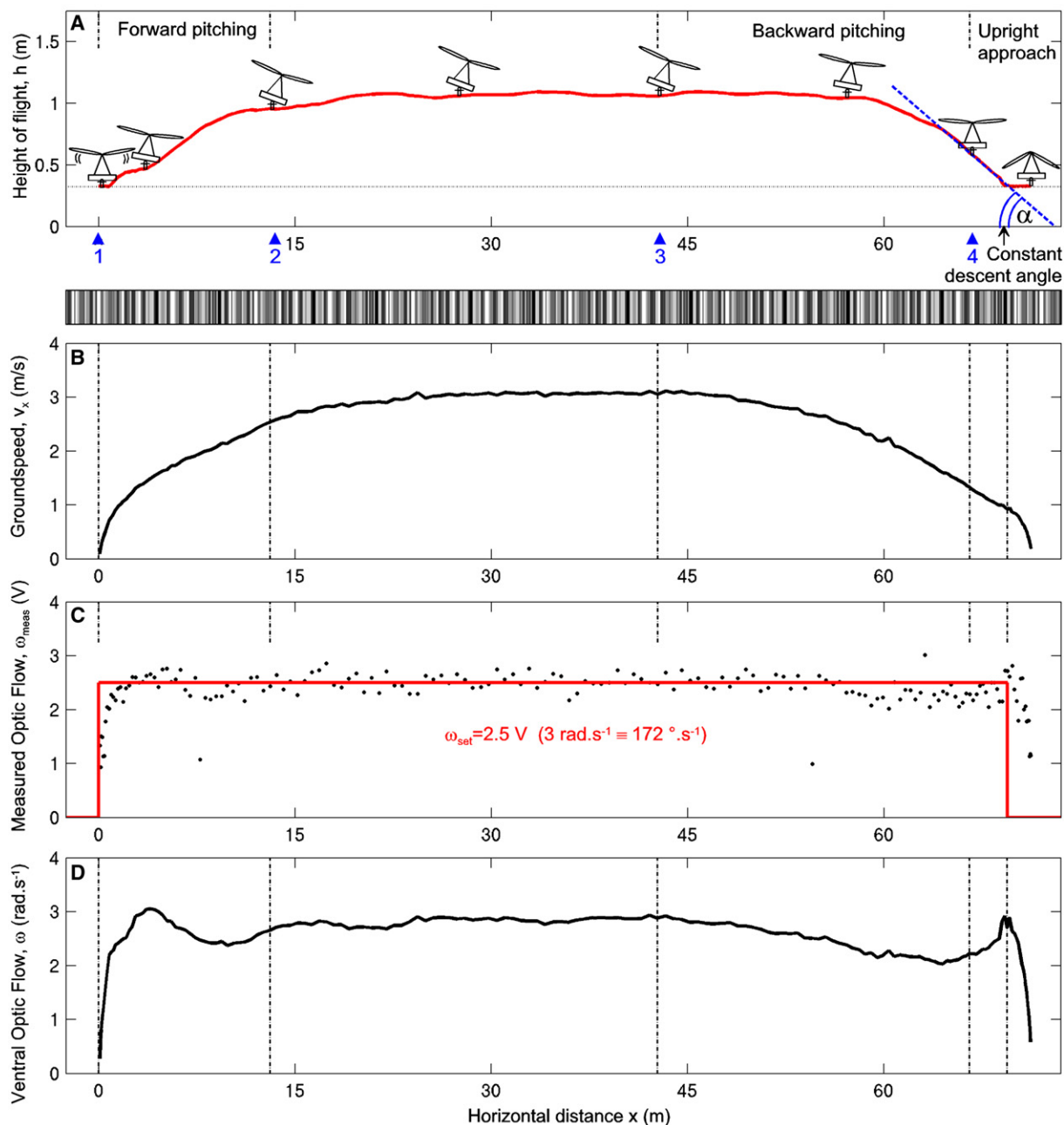
Figure 3. Flight Parameters Monitored during a 70 m Flight Performed by the Robotic Micro-Helicopter Equipped with an Optic-Flow Regulator as Shown in Figure 2

The flight consisted of about six laps. The complete journey (over the randomly textured pattern shown in [A]) includes take-off, level flight, and automatic landing.

(A) Vertical trajectory in the longitudinal plane. On the left, the operator simply pitched the MH forward rampwise by an angle $\Delta\Theta$ = +10° (between arrowheads 1 and 2). The ensuing increase in groundspeed (up to 3 m/s; see [B]) automatically triggered a proportional increase in groundheight: the MH climbed and flew level at a groundheight of approximately 1 m, as dictated by the OF set-point (ω_{set} = 3 rad/s, i.e., 172°/s, i.e., 2.5V as shown in [C]). After flying 42 m, the MH was simply pitched backward rampwise by an opposite angle $\Delta\Theta$ = −10° (between arrowheads 3 and 4), and the ensuing deceleration (see [B]) automatically initiated a proportional decrease in groundheight until landing occurred. During the final approach, which started when the MH had regained its completely upright position (arrowhead 4), the robot can be seen to have flown at a constant descent angle, as also observed in bees' landing performances [2]. Because the landing gear maintains the robot's eye 0.3 m above ground (dotted horizontal line), touchdown occurs shortly before the groundspeed v_x has reached zero, and the MH ends its journey with a short ground run.

(B) Groundspeed v_x was monitored throughout the journey.

(C) Output ω_{meas} of the OF sensor was monitored throughout the journey and shows the relatively small deviation from the OF set-point ω_{set} (in red); one exception is during the transient initial and final stages.

(D) Output ω (calculated as v_x/h) of the feedback loop. This ventral OF resulting from the MH flight pattern was held relatively—but not perfectly—constant throughout the journey.

Although a single trajectory is shown in (A), all the take-offs, level flights, and terrain-following and landing maneuvers analyzed were found to be extremely reliable and never led to any crashes [4].

groundheight (of around 1 m: Figure 3A), depending on the OF set-point (ω_{set} = 3 [rad·s^{-1}]: Figure 3C). A local increase in relief altitude constituting a "disturbance" triggers an increase in flight altitude and thus maintains a constant groundheight, which corresponds to terrain-following behavior (see Figure 2A). In a previous study, we reported that the MH flew higher at higher speeds and automatically cleared a shallow slant (see Figure 8 in [18]). An insect equipped with a similar OF regulator would therefore automatically follow the underlying ground (or canopy). The insect's OF set-point ω_{set} might depend on either innate, internal, or external factors.

3. Flight against Wind

Migrating insects have long been known to descend under headwind and ascend during lull [6, 15]. Locusts flying upwind rise and fall in inverse proportion to the rise and fall of the windspeed [6]. Likewise, dung beetles fly lower against a strong headwind than with a light headwind, and they fly higher with a strong tailwind than with a light tailwind [17]. The finding that a headwind caused bees to fly closer to the ground at reduced speed enabled Bräuninger to accompany them all the way to their nectar source ([1]; see also [19]).

Windspeed constitutes the second main type of disturbance affecting the OF autopilot. As shown in Figure 2A, when a headwind reduces the groundspeed v_x, the feedback loop will decrease the groundheight h proportionately. This characteristic accounts not only for the field data cited above but also for the response of the MH to an artificial headwind: the MH gradually lost height, but rose again upon reaching still air. When the windspeed increased, the MH landed smoothly (see Figure 13 in [4]). This finding is highly reminiscent of what occurs in many insects, which descend by headwind and settle when the wind grows stronger [5, 6, 15].

4. Flight over Mirror-Smooth Water

In one study, bees crossing mirror-smooth water during foraging trips flew lower and lower until crashing head-first into the water [3]. This did not happen, however, when the water surface was rippled or when a floating bridge provided a visual contrast. Recent studies on bees trained to fly across a lake to a food source do not quite confirm these early results [20], but the lake may not have been as ripple-free as the smaller flooded quarry used in the original experiments.

A featureless expanse of water no longer provides the animal's eye with any contrasting components, and the OF sensor will no longer respond. If ω_{meas} = 0 (Figure 2A), the error signal ε becomes large and negative, leading to a decrease in groundheight h. An OF regulator therefore accounts for the puzzling finding that bees plunge straight into calm water en route to their nectar source. The closed feedback loop irrevocably pulls the insect down whenever the OF sensor fails to respond. A similarly disastrous tendency was observed in the MH when we introduced a lack of contrast on the ground.

5. Landing

Video recordings of honeybees' grazing landings show that these insects land with a constant slope on a flat surface [2]. Bees are assumed to meet two requirements to be able to land smoothly: "(i) adjusting the speed of
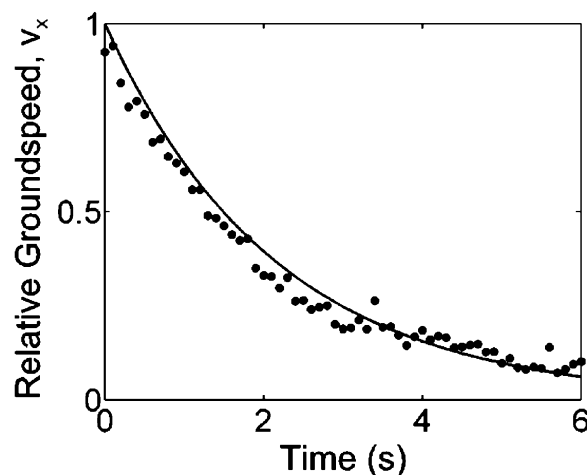

Figure 4. Decrease in Groundspeed with Time after the Cruising Robot Has Been Pitched Back to the Upright Position, i.e., during the Final Approach

The final approach starts at arrow 4 in Figure 3A. The continuous curve shows an exponential fit, from which the MH's surge time constant τ_{MH} can be estimated (τ_{MH} = 2.15 s). In the OF-regulator scheme (Figure 2), this (natural) exponential decrease in groundspeed causes a proportional decrease in the descent speed and thus leads to a constant descent slope (see text and the section "Honeybee's and Micro-Helicopter's Landing at a Constant Slope" in the Supplemental Data).

forward flight to hold constant the angular velocity of the image of the surface as seen by the eye, (ii) making the speed of descent proportional to the forward speed" [2]. Our OF-based feedback scheme adjusts not the forward flight speed but the vertical lift and makes the bee automatically land with a constant slope.

The MH's and the bee's landing behavior can be explained on the same basis because the surge dynamics can be described in both cases by similar first-order linear differential equations (see the section "Honeybee's and Micro-Helicopter's Surge Dynamics" in the Supplemental Data).

Landing is initiated by a command for the MH to gradually pitch backward to the vertical (at arrowhead 3 in Figure 3A). The ensuing deceleration automatically initiates landing because the groundheight is bound to decrease proportionally to the groundspeed. The final approach starts when the MH reaches the upright position (arrow 4 in Figure 3A). From this moment onward, v_x decreases exponentially with the "surge time constant" τ_{MH} (Figure 4), and the feedback loop forces h and its derivative dh/dt (i.e., the descent speed v_z) to decrease with the same time constant. The descent speed:groundspeed ratio v_z:v_x, i.e., the descent slope, will therefore remain constant throughout the final approach, as actually observed both in landing bees [2] and in the landing MH (Figure 3A).

As shown in the section "Honeybee's and Micro-Helicopter's Landing at a Constant Slope" in the Supplemental Data, the ensuing descent angle α[rad.] can be calculated as follows:

$$\alpha = -\arctan(1/(\omega_{set}\tau)) \qquad (3)$$

where ω_{set} = OF set-point [rad·s^{-1}], and τ = surge time constant [s] (τ_{MH} = 2.15 s, Figure 4).

If the constant-slope landing glide of bees reflects the presence of an OF regulator in these insects, then by substituting the bees' landing data ($\alpha_{BEE} = -28°$, $\omega_{setBEE} = 500°$/s [2]) into Equation 3, we obtain the bee's *surge time constant*:

$$\tau_{BEE} = 0.22s$$

Srinivasan et al. measured an exponential decrease in groundheight with time [2]. From their data on four bees (Figure 8 in [2]), we calculated time constants of 0.22 s, 0.27 s, 0.29 s, and 0.57 s. These values closely match the value $\tau_{BEE} = 0.22$ s predicted by our model.

Conclusion

Here we have described an explicit control scheme, that of the optic-flow regulator controlling the lift (Figure 2A); this optic-flow regulator may explain how insects manage to fly safely over a contrasting ground. Unlike classical aircraft autopilots, which involve "altitude-holding" or "speed-holding" abilities, our visually based control scheme is a remarkably novel type of autopilot that involves "OF holding," with the interesting effect that the groundheight becomes automatically proportional to the groundspeed. This control scheme may enable insects to deal single handedly with all maneuvers, such as taking off, flying at a level height, landing, and responding appropriately to wind, without being informed about groundheight, groundspeed, airspeed, windspeed, or ascent or descent speed, and hence without any need for the metric sensors with which conventional aircraft are equipped. In view of the relatively constant OF ω maintained throughout the journey (see Figure 3D), few constraints are imposed on the OF sensor, which needs only to detect any deviations from the OF setpoint and therefore requires only a small OF range.

Whether an insect's deceleration results from its intention to land (section 5) or from the braking effects of a strong headwind (section 3), the feedback loop will always ensure smooth touchdowns because it pulls the insect down at a rate that is no faster than that of the decrease in groundspeed. During both take-off and landing, the closed visual-feedback loop will compensate for any disturbances, such as uneven terrain, wind gusts, and ground effects.

Our model differs from another one where the OF controls the groundspeed v_x rather than the groundheight h [2, 10, 21, 22]. Controlling v_x instead of h in Figure 2A would, however, produce strikingly different flight patterns from those reported by previous authors, as follows:

(i) Instead of following a slanting terrain, as migrating butterflies [15, 16] and our MH [4, 18] do, insects would gradually decelerate until touching the rising slope at a negligible speed and would thus inopportunely interrupt their journey.

(ii) Instead of descending in a headwind and rising in a tailwind, as honeybees [1, 19], locusts [6], dung beetles [17], mosquitoes [5], and our MH [4] do, insects would compensate for the unfavorable headwind by increasing their airspeed without changing their groundheight.

These two models can be reconciled, however, if we add to our own model the hypothesis that a second OF regulator may be in charge of adjusting the groundspeed by regulating the lateral OF [39]. Experiments on tethered [23, 24] and free-flying flies [7, 25, 26] and bees [10, 22], as well as on tethered locusts [27], have long shown that motion detected in the lateral part of the eyes affects the forward thrust, and hence the forward speed. In short, this additional hypothesis amounts to saying that the panoramic compound eye is subdivided into a ventral region and a lateral *region*, each of which is responsible for measuring the OF for a specific OF regulator: a ventral OF regulator controlling the vertical lift (and thus the groundheight), as suggested above, and a lateral OF regulator controlling the forward thrust (and thus the airspeed).

The control scheme presented in Figure 2A is not meant to describe the underlying neural circuits in any detail, but its neural implementation is not very demanding. This explicit model lays the groundwork for future electrophysiological experiments because it is easier to identify a neural circuit with a specific functional scheme in mind. Figure 2A describes the causal links between visual and motor variables in a concise two-dimensional block diagram, which also includes the dynamic aspects. One can use this scheme to translate the signal-processing principles into other technological terms: into electronic terms, for example, as we did in our MH. While harnessing biological principles to design smart autonomous vehicles, biorobotics also provides biology with fair returns: physical reconstruction of a biological process is yet another path toward discovery [28–30].

Experimental Procedures

Micro-Helicopter
The tethered micro-helicopter (MH) and its arena have been described in previous robotics studies [4, 18], and we will therefore describe them only briefly here. Our proof-of-concept MH has a fixed-pitch rotor (diameter 30 cm, mass 5 g), the rotational speed of which determines the rotor thrust, and hence the mean flight force F (Figure 2B).

Optic-Flow Sensor
The 2.5 g ventral eye of the MH keeps pointing vertically downward. It is composed of a miniature lens (focal length 8.5 mm) and a pair of photoreceptors driving a single EMD (Figure 1B), an electro-optic angular-velocity sensor (mass $\approx$ 0.5 g) based on findings made on the fly's elementary motion detector (EMD) [31, 32] when the responses of a motion-detecting neurone to optical microstimulation applied to two single photoreceptor cells within a single ommatidium were recorded [33]. This OF sensor detects all motion occurring within a one-decade angular speed range (from 40°/s to 400°/s), whatever the spatial frequency and the level of contrast (down to about 0.04).

Flight Arena
The 100 g MH is tethered to the tip of a light panthographic arm (radius 1.9 m) that is free to rotate frictionlessly about a central pole [4, 18]. The MH provides its own lift and is free to circle around with an unhindered, unlimited course over a flat surface (average track length per lap = 12 m) covered with a richly contrasting, one-dimensional computer-printed pattern with a random spatial wavelength λ ($0.57° < \lambda < 16.7°$ at $h = 1$ m) and a random contrast m ($0.04 < m < 0.3$) (a linear development of this pattern is shown at the bottom of Figure 3A). Headwind conditions were simulated with a fan oriented tangentially to the circular MH track.

Flight Monitoring

The MH's flight trajectory in the longitudinal plane (defined in Figures 1A and 3A) is monitored in real time via ground-truth sensors (a servo-grade miniature potentiometer for the elevation and an optical encoder for the azimuth) mounted on the rotational axes of the supporting arm. The angular measurements are converted into groundheight h, horizontal distance x, and groundspeed v_x (Figures 3A and 3B). The OF signal measured (Figure 3C) is the output signal (in volts) from the OF sensor.

Operation

Forward acceleration is initiated when the operator remotely commands the MH to gradually pitch forward by a few degrees (Figure 2B). The MH reacts to the ensuing ventral OF by controlling the rotor speed, and hence the mean flight-force amplitude F (Figure 2B), which determines the vertical lift L, and hence the groundheight h, so as to keep the ventral-OF measured ω_{meas} equal to the OF set-point ω_{set} (Figure 2A). Controlling F might be expected to affect not only L but also T (Figure 2B). This coupling is negligible, however, because the change in T is much smaller than the change in L (by a factor of at least $5.67 = \mathrm{cotan}(10°)$ because Θ never exceeds $+10°$) and much slower than the change in L (by a factor 3.2 = ratio of the open-loop rising time of T and closed-loop rising time of L).

MH versus Insects

Although our MH is much simpler than any insect, it has many insect-like characteristics (ocular interreceptor angle: $\Delta\varphi = 4.2°$; acceptance angle of each photoreceptor bell-shaped angular sensitivity function, $\Delta p = 4.2°$ groundheight range: 0–3 m; flight speed range: 0–3 m/s; OF sensor range: 40°/s to 400°/s). Its surge dynamics are about ten times slower than those of the honeybee, however.

Supplemental Data

Supplemental Data include additional Results and are available online at http://www.current-biology.com/cgi/content/full/17/4/■ ■ ■/DC1/.

References

1. Bräuninger, H.D. (1964). Über den Einfluss meteorologischer Faktoren auf die Entfernungsweisung im Tanz der Bienen. Z. Vergl. Physiol. 48, 1–130.

2. Srinivasan, M.V., Zhang, S., Chahl, J.S., Barth, E., and Venkatesh, S. (2000). How honeybees make grazing landings on flat surfaces. Biol. Cybern. 83, 171–183.

3. Heran, P., and Lindauer, M. (1963). Windkompensation und Seitenwindkorrektur der Bienen beim Flug über Wasser. Z. Vergl. Physiol. 47, 39–55.

4. Ruffier, F., and Franceschini, N. (2005). Optic flow regulation: The key to aircraft automatic guidance. Rob. Auton. Syst. 50, 177–194.

5. Kennedy, J.S. (1939). Visual responses of flying mosquitoes. Proc. Zool. Soc. Lond. 109, 221–242.

6. Kennedy, J.S. (1951). The migration of the desert locust (Schistocerca gregaria Forsk.) I. The behaviour of swarms. Philos. Trans. R. Soc. Lond. B 235, 163–290.

7. David, C. (1982). Compensation for height in the control of groundspeed by Drosophila in a new 'Barber's pole' wind tunnel. J. Comp. Physiol. A147, 485–493.

8. Kirchner, W.H., and Srinivasan, M.V. (1989). Freely moving honeybees use image motion to estimate distance. Naturwiss. 76, 281–282.

9. Srinivasan, M.V., Lehrer, M., Kirchner, W.H., and Zhang, S. (1991). Range perception through apparent image speed in freely flying honeybees. Vis. Neurosci. 6, 519–535.

10. Baird, E., Srinivasan, M.V., Zhang, S., and Cowling, A. (2005). Visual control of flight speed in honeybees. J. Exp. Biol. 208, 3895–3905.

11. Ibbotson, M.R. (2001). Evidence for velocity-tuned motion-sensitive descending neurons in the honeybee. Proc. R. Soc. Lond. B. Biol. Sci. 268, 2195–2201.

12. Shoemaker, P.A., O'Caroll, D.C., and Straw, A.D. (2005). Velocity constancy and models for wide-field visual motion detection in insects. Biol. Cybern. 93, 275–287.

13. David, C. (1978). The relationship between body angle and flight speed in free-flying Drosophila. Physiol. Entomol. 3, 191–195.

14. Esch, H., Nachtigall, W., and Kogge, S.N. (1975). Correlations between aerodynamic output, electrical activity in the indirect flight muscles and wing positions of bees flying in a servomechanically controlled flight tunnel. J. Comp. Physiol. 100, 147–159.

15. Williams, C.P. (1965). Insect Migration, Second Edition (London: Collins).

16. Srygley, R.B., and Oliveira, E.G. (2001). Orientation mechanisms and migration strategies within the flight boundary layer. In Insect Movements: Mechanisms and Consequences, T.P. Woiwod, D.R. Reynolds, and C.D. Thomas, eds. (Wallingford, Oxon, UK: CABI Publishing, CAB International), pp. 183–206.

17. Steiner, G. (1953). Zur Duftorientierung fliegender Insekten. Naturwiss. 19, 514–515.

18. Ruffier, F., and Franceschini, N. (2003). A bioinspired visuomotor control system for the guidance of micro-air vehicles. In Bioengineered and Bioinspired Systems, Volume 5119, A. Rodriguez-Vasquez, D. Abbott, and R. Carmona, eds. (Bellingham, WA: SPIE [The International Society for Optical Engineering]), pp. 1–12.

19. Riley, J.R., and Osborne, J.L. (2001). Flight trajectories of foraging insects: Observations using harmonic radar. In Insect movement: Mechanisms and Consequences, T.P. Woiwod, D.R. Reynolds, and C.D. Thomas, eds. (Wallingford, Oxon, UK: CABI Publishing, CAB International), pp. 129–157.

20. Tautz, J., Zhang, S., Spaethe, J., Brockman, A., Si, A., and Srinivasan, M. (2004). Honeybee odometry: Performance in varying natural terrain. PLoS Biol. 2, e211.

21. Preiss, R., and Kramer, E. (1984). Control of flight speed by minimization of the apparent ground pattern movement. In Localization and Orientation in Biology and Engineering, D. Varju and H. Schnitzler, eds. (Berlin: Springer), pp. 140–142.

22. Srinivasan, M.V., Zhang, S., Lehrer, M., and Collett, T. (1996). Honeybee navigation en route to the goal: Visual flight control and odometry. J. Exp. Biol. 199, 237–244.

23. Götz, K.G. (1968). Flight control in Drosophila by visual perception of motion. Kybernetik 4, 199–208.

24. Götz, K.G., and Buchner, E. (1978). Evidence for one-way movement detection in the visual system of Drosophila. Biol. Cybern. 31, 243–248.

25. David, C. (1979). Height control by free-flying Drosophila. Physiol. Entomol. 4, 209–216.

26. David, C. (1985). Visual control of the partition of flight force between lift and thrust in free-flying Drosophila. Nature 313, 48–50.

27. Spork, P., and Preiss, R. (1993). Control of flight by means of lateral visual stimuli in gregarious desert locusts. Physiol. Entomol. 18, 195–203.

28. Franceschini, N., Pichon, J.M., and Blanes, C. (1992). From insect vision to robot vision. Philos. Trans. R. Soc. Lond. B 337, 283–294.

29. Webb, B. (2001). Can robots make good models of biological behaviour? Behav. Brain Sci. 24, 1033–1050.

30. Franceschini, N. (2003). From insect vison to robot vision: Reconstruction as a mode of discovery. In Sensors and Sensing

in Biology and Engineering., F.G. Barth, J.A. Humphrey, and T.W. Secomb, eds. (Berlin: Springer), pp. 223–235.

31. Blanes, C. (1986). Appareil visuel élémentaire pour la navigation à vue d'un robot mobile autonome. MS in Neuroscience (Marseille, France: University of Aix-Marseille II).

32. Franceschini, N., Blanes, C., and Oufar, L. (1986). Passive non-contact optical velocity sensor, (in French). Dossier technique N° 51549 (Paris: Agence Nationale pour la Valorisation de la Recherche/Direction de la Valorisation).

33. Franceschini, N. (1985). Early processing of color and motion in a mosaic visual system. Neurosci. Res. (*Suppl. 2*), 17–49.

34. Vogel, S. (1967). Flight in *Drosophila* I/ Flight performance of tethered flies. J. Exp. Biol. *44*, 567–578.

35. Götz, K.G., and Wandel, U. (1984). Optomotor control of the force of flight in *Drosophila* and *Musca*. II, Covariance of lift and thrust in still air. Biol. Cybern. *51*, 135–139.

36. Zanker, J. (1985). On the mechanism of speed and altitude control in *Drosophila melanogaster*. Physiol. Entomol. *13*, 351–361.

37. Dickinson, M., and Götz, K.G. (1996). The wake dynamics and flight forces of the fruit fly *Drosophila melanogaster*. J. Exp. Biol. *199*, 2085–2104.

38. Ellington, C.P. (1984). The aerodynamics of hovering insect flight. V/A vortex theory. Philos. Trans. R. Soc. Lond. B Biol. Sci. *305*, 115–144.

39. Serres, J., Ruffier, F., and Franceschini, N. (2006). Two optic flow regulators for speed control and obstacle avoidance. Proc. IEEE Int. Conf. On Biomedical Robotics and Biomechatronics, Pisa, Italy, paper no 284.